nature geoscience

LETTERS

PUBLISHED ONLINE: 8 SEPTEMBER 2013 | DOI: 10.1038/NGEO1928

Eruption cyclicity at silicic volcanoes potentially caused by magmatic gas waves

Chloé Michaut[1]*, Yanick Ricard[2], David Bercovici[3] and R. Steve J. Sparks[4]

Eruptions at active silicic volcanoes are often cyclical. For example, at the Soufrière Hills volcano in Montserrat[1], Mount Pinatubo in the Philippines[2], and Sakurajima in Japan[3], episodes of intense activity alternate with repose intervals over periods between several hours and a day. Abrupt changes in eruption rates have been explained with the motion of a plug of magma that alternatively sticks or slides along the wall of the volcanic conduit[4,5]. However, it is unclear how the static friction that prevents the plug from sliding is periodically overcome. Here we use two-phase flow equations to model a gas-rich, viscous magma ascending through a volcanic conduit. Our analyses indicate that magma compaction yields ascending waves comprised of low- and high-porosity bands. However, magma ascent to lower pressures also causes gas expansion. We find that the competition between magma compaction and gas expansion naturally selects pressurized gas waves with specific periods. At the surface, these waves can induce cyclical eruptive behaviour with periods between 1 and 100 hours, which compares well to the observations from Soufrière Hills, Mount Pinatubo and Sakurajima. We find that the period is insensitive to volcano structure, but increases weakly with magma viscosity. We conclude that observations of a shift to a longer eruption cycle imply an increase in magma viscosity and thereby enhanced volcanic hazard.

Periodic cycles of ground deformation, seismicity and eruptive activity have been recorded at a number of active silicic volcanoes, most notably at the Soufrière Hills volcano (SHV), Montserrat, in 1996–1997, Mount Pinatubo, Philippines, in 1991 (Fig. 1) and Showa crater, Sakurajima volcano, Japan, in 2008–2010. Recurrent inflation and deflation of SHV (inferred by tilt measurements) with periods between 6 and 30 h were accompanied by seismic swarms (Fig. 1). This pattern persisted for months during 1996–1997 (ref. 1). The cycle peaks correlated with significant eruptive events, such as pyroclastic flow instabilities, explosive vulcanian eruptions or rapid dome growth. Measurements of ground deformation were used to predict time of increased volcanic hazards[6]. From 21 September to 22 October 1997, 74 vulcanian explosions occurred with an average periodicity of 10 h (ref. 7).

Following the 1991 Mount Pinatubo eruption, low-frequency seismicity increased and developed into discrete periodic events 7–10 h long (Fig. 1), similar to the periodicity recorded at SHV. Periodic seismic activity was also long-lasting and often accompanied by intermittent explosive activity[2]. At Sakurajima, repetitive vulcanian explosions with a timescale of hours are also associated with precursory inflation and seismicity[3].

During both the Pinatubo and SHV eruptive events, tilt and seismic amplitudes decreased rapidly with distance from the summit[1,2], suggesting a shallow pressure source probably located in the volcanic conduit. At SHV and Sakurajima, the pressure source depth is estimated to be of several hundreds of metres up to 2 km on the basis of the comparison of tilt data with deformation models along with petrological studies of deposits[6,8] or on strain meter data[3].

Different competing mechanisms have been proposed to explain cyclicity. Previous work suggests that whereas volatile exsolution and microlite crystallization lead to rheological stiffening of the magma, which resists extrusion, gas pressurization below this plug drives extrusion and explosive activity[1]. Other models propose a competition between gas escape, which reduces the flow pressure, and gas exsolution, which increases it[9]. Fluxes in SO_2 release increased with inflation amplitude at SHV, suggesting that gas accumulation provided the pressure source[10,11]. At Sakurajima, the inflation ended with a gradual decrease in SO_2 emission over several hours before an explosion, indicating a simultaneous pressure increase due to gas and magma accumulation at depth along with sealing of a surface magma layer[3].

Stick–slip behaviour of a stiffened plug sliding along the conduit walls and driven by pressure build-up at depth in the compressible magma is a popular mechanism to explain abrupt changes in eruption rate at silicic volcanoes[4,5]. When the ratio between the driving pressure in the magma below the plug and the normal stress exceeds the static friction, slip begins and the driving pressure decreases until it drops below the slip surface strength and the plug sticks again[4,5]. This plug mechanism leads to a wide range of oscillatory patterns but does not predict a specific and regular period. Various mechanisms have been added to the plug model to explain the observed repetitive cycles of hours to days, including magma compression forced by influx into the conduit[4], volatile diffusion from supersaturated melt into gas bubbles[5] and elastic wall deformation[5]. However, after an explosion, the thick plug is disrupted and the models require its rapid regeneration to explain the occurrence of the following cycle. Magma cooling is far too slow; thus, degassing is probably involved in plug formation[8] although the implied formation time is unknown. Furthermore, in most models, the predicted periodicity is related to conduit and plug geometry and slip surface strength[4]. However, time-dependent effects such as conduit erosion, wall heating by friction, or even dome collapse[1] should lead to large variations in cycle frequency, which are not observed. In addition, conduit and plug geometries probably differ from one volcano to the next. A challenge is thus to explain both the

[1]Laboratoire de Sciences Spatiales et Planétologie, Université Paris Diderot, Sorbonne Paris Cité, Institut de Physique du globe de Paris, UMR 7154 CNRS, F-75013 Paris, France, [2]Laboratoire de Géologie de Lyon, UMR 5276 CNRS, Université Lyon 1, ENS Lyon, 69622 Villeurbanne, France, [3]Department of Geology and Geophysics, Yale University, New Haven, Connecticut 06520-8109, USA, [4]Department of Earth Sciences, Wills Memorial Building, University of Bristol, Bristol BS8 1RJ, UK. *e-mail: michaut@ipgp.fr

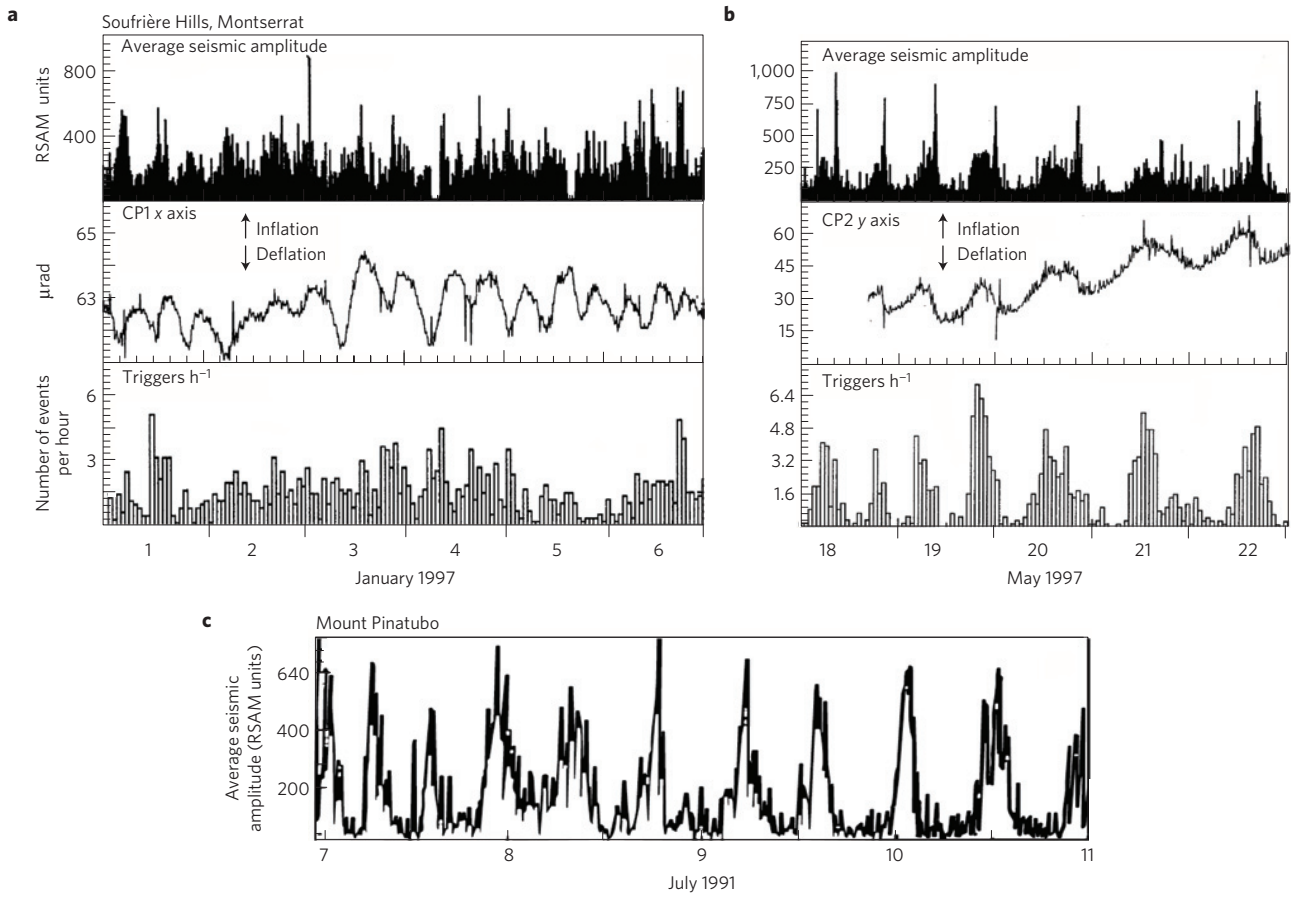

Figure 1 | Observed cyclicity at two different silicic volcanoes. a,**b**, Cycles recorded at the Soufrière Hills volcano, Montserrat, modified from ref. 1. Cyclic deformation of the edifice indicated by tilt meters installed on Chances Peak (CP1 and CP2) correlates with real-time seismic amplitude measurements (RSAM) and triggered earthquakes with an average periodicity of ~6 to >20 h, in January (**a**) and May (**b**) 1997. **c**, Low-frequency seismic activity at Mount Pinatubo, July 1991, shows a periodicity of 7–10 h, modified from ref. 2.

regularity of repetitive sequences of dome growth and explosion, despite changes in volcano structure, and the occurrence of a comparable periodicity range at a number of different volcanoes[2,6,12,13].

Here we show that gas waves of growing amplitude and specific wavelengths and periods are naturally produced in an ascending gas-rich viscous magma by the competition between magma compaction, which squeezes the pore space, and gas expansion during ascent (Fig. 2).

Gas segregation from magma is controlled by gas buoyancy, resistance to gas percolation through magma and deformation of the magma matrix, or magma compaction, which squeezes the pore space. Compaction has mainly been used to study melt expulsion from partially molten mantle, with two incompressible phases[14,15]. The application of two-phase physics to vesicular magma shows that compaction expels gas (if assumed incompressible) from regions that are 1–10 times the compaction length[14–16]:

$$\delta = \sqrt{\frac{\mu_m k_0}{\mu_g}} \qquad (1)$$

where μ_m and μ_g are magma and gas viscosities and k_0 is a reference permeability; this expression assumes that permeability is dependent on gas volume fraction ϕ according to $k(\phi) = k_0\phi^n$ with $n = 2$ (different values of n do not alter our results; Supplementary Information). The compaction length reaches 1–15 m, for $\mu_m = 10^7$–10^{10} Pa s and $k_0 = 10^{-13}$–10^{-12} m^2 (see ref. 16). In general, compaction expels lighter fluid from a mixture in the form of buoyant pulses or solitary waves with higher fluid content; but, in the absence of fluid compressibility, these waves neither grow nor decay; thus, no unique wavelength is naturally selected from all possible excited waves[14,16].

However, in a bubbly magma, gas is highly compressible; thus, gas pulses can grow or decay by gas expansion or compression. For short waves, stresses from magma compaction, which act to squeeze out fluid, are large enough to compress the gas and thus damp the waves. For longer waves, compaction is weaker, permitting gas expansion and wave growth during ascent; however, for very long waves, the pulse volume is spread out and the gas can escape, leading to weaker pulse growth. Wave growth is therefore maximized at an intermediate wavelength, which is associated with a dynamically favourable wave; the surface oscillations induced by this wave possibly lead to the observed periodicity.

Solving the mass and momentum conservation equations for the two phases and linearizing to first order leads to a dispersion relation describing the growth rate and velocity of the unstable wave as a function of its wavelength $\mathcal{L}$ (Supplementary Information). When gas expansion is neglected, the wave growth rate is uniformly zero, whereas when compaction is neglected, all waves grow equally by expansion (Fig. 3a); in neither case is there a preferred, selected, wave. When both gas compression and magma compaction are considered, a maximum growth occurs at a particular wavelength $\mathcal{L}_{max}$ that delineates the dominant wave.

The value of $\mathcal{L}_{max}$ is controlled by three dimensionless parameters: the background gas fraction ϕ_0, the background gas to

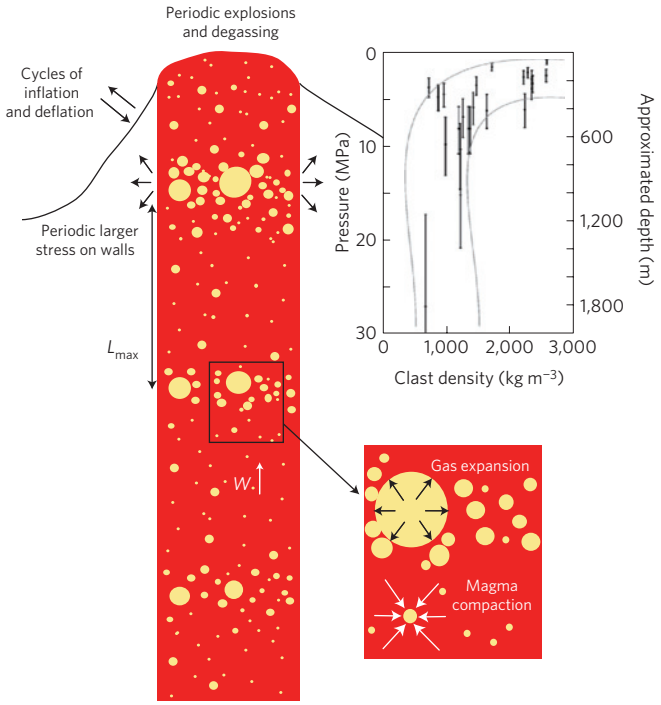

Figure 2 | Alternation between gas-rich and degassed magma layers. The competition between compaction and gas expansion induces unstable waves of gas in volcanic conduits and periodic behaviour at the surface. The shortest perturbation wavelength $\mathcal{L}$ is 100 to 1,500 m, resulting in a surface periodicity $\mathcal{L}/\mathcal{W}$ of 1–100 h, with $\mathcal{W}=10$–50 m h^{-1}, the magma ascent velocity. Right: at SHV, the observations of clast density versus depth before eruption (quench pressure) suggest the presence of a gas-rich layer at depth and porosity variations over a length scale comparable to the predicted selected wavelength, modified from ref. 8.

magma density ratio ρ_0/ρ_m and most importantly the ratio between the characteristic pressure in the expanding gas ($\rho_m C_g^2$, where C_g is gas sound speed) and the characteristic pressure exerted on the gas by compaction ($\rho_m g\delta$, where g is gravity and δ is compaction length given by (1)), noted $\beta = C_g^2/g\delta$. However, the growth rate shows a broad maximum with a dominant wavelength range that stays between $\sim 10^2\delta$ and $10^3\delta$ despite large changes in the parameters (Fig. 3 and Supplementary Fig. S2). Hence, for δ between 1 and 15 m, the shortest gas wave that can expand freely has a wavelength between 100 and 1,500 m (Fig. 3).

To study the system's full nonlinear evolution over the conduit length, we numerically solved the conservation equations. Calculations confirm the linear theory and show that, in the compressible-gas case, waves with wavelengths of a few hundred δ quickly become dominant over all possible fluctuations (Fig. 4) and grow over the conduit length. Similar waves with a dominant wavelength occur in a flow of suspended bubbles in magma, as opposed to permeable magma, demonstrating the robustness of this process. Calculations also show that the same wavelength range is selected when accounting for gas exsolution proceeding at thermodynamic equilibrium (Supplementary Information).

Overall, given natural fluctuations in gas and magma flux, our proposed mechanism should select waves with wavelengths between 100 and 2,000 m depending on magma viscosity (Figs 3 and 4). The wave speed is close to the eruption velocity (Supplementary Information), which generally averages 10–50 m h^{-1} as for SHV in 1996–1997 (ref. 1). These wavelengths correspond to periods of $\sim$1 to 100 h between gas pulse arrivals at the surface (Fig. 3b), depending on magma viscosity and ascent rate, which is the typical periodicity observed in Montserrat, Mount Pinatubo and Sakurajima. Gas overpressure oscillates with the same periodicity (Fig. 4). Moreover, changes in the observed periodicity are associated with magma viscosity variations at SHV, as predicted by our theory. Before 15 July 1996, effusive activity at SHV was characterized by extrusions of spines and whalebacks, whereas vigorous extrusion of much less viscous magma occurred from mid-July to September 1996 (ref. 17); indeed this episode showed a decrease in the seismic pattern periodicity, from days down to several hours[18]. During early January 1997, the periodicity recorded by tilt meters was the shortest on average, 6–8 h (ref. 1; Fig. 1) and the extruding lobe exhibited the most fluid behaviour[17]. Then in May 1997, a large vertical spine erupted and the period was larger than average, that is 12 to >20 h (Fig. 1), even though the eruption rate was similar to that in January[18].

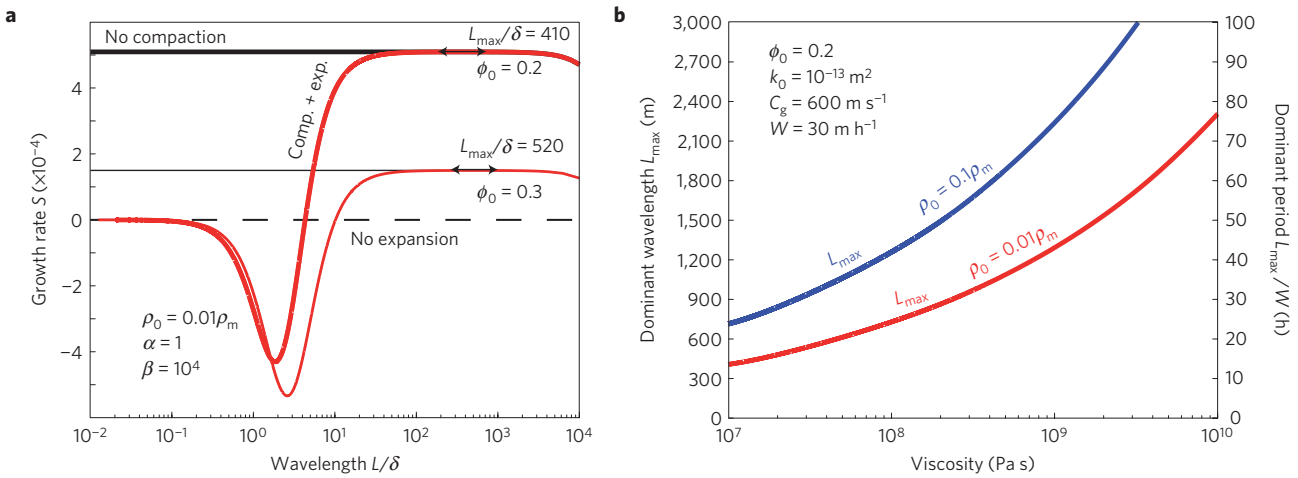

Figure 3 | Dominant wavelength of the perturbation predicted by the theory. a, Growth rate normalized by δ/W versus wavelength of the perturbation for two different values of ϕ_0. Without magma compaction, the growth is independent of wavelength (solid black lines). Without gas expansion, the growth rate is zero (horizontal dashed line). The range of dominant wavelengths is $10^2\delta$–$10^3\delta$. We use $\mu_m = 10^7$–10^{12} Pa s, $\mu_g = 10^{-5}$ Pa s and $k_0 = 10^{-13}$–10^{-12} m^2 (refs 16,21,22); hence, $\delta \sim$ 1–15 m, $\rho_0 \sim$ 10–500 kg m^{-3}, $\rho_m = 2{,}500$ kg m^{-3} and $C_g = 600$–700 m s^{-1}; hence $\beta = g\delta/C_g^2 = 5\times10^2$–$5\times10^4$ and $\alpha = (\mu_g\mathcal{W})/(k_0\rho_m g) = 0.1$–$100$ (the parameter α only slightly plays on the instability growth rate; Supplementary Information). **b**, Dominant wavelength and period as a function of viscosity.

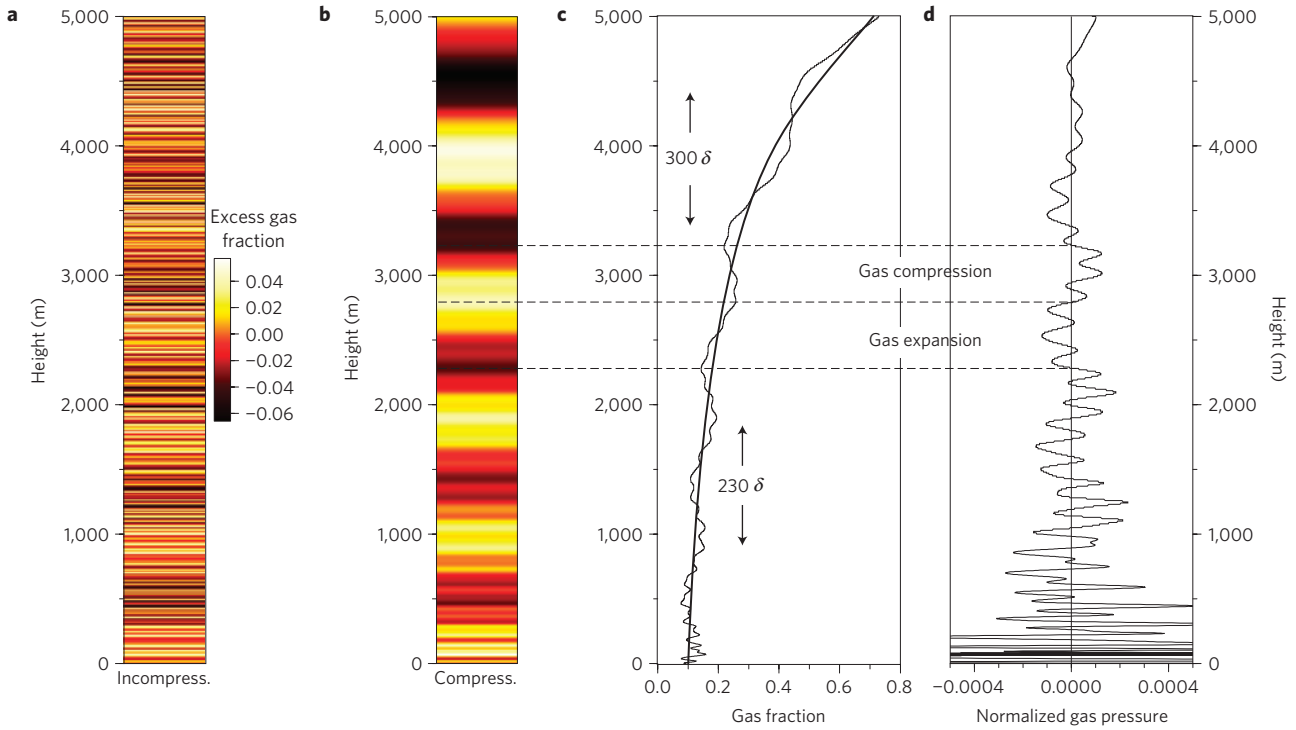

Figure 4 | Gas fraction and overpressure profiles obtained from numerical calculations. The time-dependent basal gas fraction is a sum of 7 sinusoidal perturbations. **a**, Excess gas fraction relative to the steady-state profile assuming incompressible gas, that is, a constant ρ_g in Supplementary Equations (1)-(4) and (8) (Supplementary Information). **b**, In the compressible gas, one wavelength, growing from 200 to 300δ, is rapidly selected. **c**, Gas fraction steady-state (thick line) and time-dependent (thin line) profiles. **d**, Gas overpressure $(P_f - P_m)/(\rho_m g\delta)$ in excess of the steady-state profile. We assume $\phi_0 = 0.1$ and $\rho_0 = 0.08\rho_m = 200\,\mathrm{kg\,m^{-3}}$ at the base, no exsolution, $\delta = 3.65$ m, $\mathcal{W} = 10\,\mathrm{m\,h^{-1}}$, $\alpha = 1.1$, $\beta = 13400$, $\mu_m = 10^8$ Pa s and $\rho_m g\delta \approx 9 \times 10^4$ Pa.

Abrupt changes in eruption rates are possibly best explained by a failure mechanism near the surface such as stick–slip rheology or magma fragmentation, which would be achieved when the critical overpressure[19] or gas fraction is reached in the conduit. The shallower gas-rich layer occurs at a depth less than one wavelength (that is, <2 km, Fig. 2) and shows a higher gas overpressure relative to the steady-state profile in its upper half (Fig. 4). This pressurized gas-rich layer could provide a preferred location for the pressure source and for earthquake nucleation through its interaction with the conduit wall or overlying plug. Furthermore, compaction of the degassed surficial magma layer provides a possible way of stiffening a surface plug. At Sakurajima, plug disruption by gas leakage a few minutes before eruption suggests a process involving gas pressure build-up to a plug failure threshold. This observation, and the reduction in SO_2 flux accompanying inflation from a pressure source depth of ~1 km, both illustrate that simultaneous shallow gas accumulation and plug formation by compaction probably drive the system[3].

The time interval between cycles of inflation, seismic swarms and eruption at SHV, Montserrat, remained remarkably consistent during its main eruptive phase in 1996–1997: between 6 and 30 h. Other silicic volcanoes such as Mount Pinatubo[2], Sakurajima volcano[3], Mount Unzen[12,20] or Mount St Helens[13] exhibit comparable oscillations of a few hours to a day. Our analysis shows that expanding gas waves with wavelength 100–2,000 m are naturally selected in ascending gas-rich silicic magma and can potentially induce such a long-period cyclicity, which would be controlled by magma viscosity and ascent rate. In contrast to other models, the predicted periodicity does not depend on surficial conditions or volcano structure, but increases moderately with magma viscosity, as observed in SHV, Montserrat[1].

Received 7 May 2013; accepted 25 July 2013; published online 8 September 2013

References

1. Voight, B. *et al.* Magma flow instability and cyclic activity at Soufrière Hills Volcano, Montserrat, British West Indies. *Science* **283,** 1138–1142 (1999).
2. Mori, J. *et al.* in *Fire and Mud: Eruptions and Lahars of Mount Pinatubo, Philippines* (eds Newhall, C. G. & Punongbayan, R. S.) 339–350 (Univ. Washington Press, 1996).
3. Yokoo, A., Iguchi, M., Tameguri, T. & Yamamoto, K. Processes prior to outbursts of vulcanian eruption at Showa Crater of Sakurajima Volcano. *Bull. Volcanol. Soc. Jpn* **58,** 163–181 (2013).
4. Denlinger, R. P. & Hoblitt, R. P. Cyclic eruptive behavior of silicic volcanoes. *Geology* **27,** 459–462 (1999).
5. Lensky, N. G., Sparks, R. S. J., Navon, O. & Lyakhovsky, V. Cyclic activity at Soufrière Hills Volcano, Montserrat: Degassing-induced pressurization and stick-slip extrusion. *Geol. Soc. Lond. Spec. Pub.* **307,** 169–188 (2008).
6. Voight, B. *et al.* Remarkable cyclic ground deformation monitored in real time on Montserrat and its use in eruption forecasting. *Geophys. Res. Lett.* **25,** 3405–3408 (1998).
7. Druitt, T. H. *et al. Volcanic Processes, Products and Hazards* 281–306 (Geol. Soc. Lond. Mem., 2002).
8. Clarke, A. B., Stephens, S., Teasdale, R., Sparks, R. S. J. & Diller, K. Petrologic constraints on the decompression history of magma prior to vulcanian explosions at the Soufrière Hills Volcano, Montserrat. *J. Volcanol. Geotherm. Res.* **161,** 261–274 (2007).
9. Connor, C. B., Sparks, R. S. J., Mason, R. M., Bonadonna, C. & Young, S. R. Exploring links between physical and probabilistic models of volcanic eruptions: the Soufrière Hills Volcano, Montserrat. *Geophys. Res. Lett.* **30,** 34.1–34.4 (2003).
10. Edmonds, S., Oppenheimer, C., Pyle, D. M., Herd, R. A. & Thompson, G. SO_2 emissions from Soufrière Hills Volcano and their relationship to conduit permeability, hydrothermal interaction and degassing regime. *J. Volcanol. Geotherm. Res.* **124,** 23–43 (2003).
11. Watson, I. M. *et al.* The relationship between degassing and ground deformation at Soufrière Hills Volcano, Montserrat. *J. Volcanol. Geotherm. Res.* **98,** 117–126 (2000).

12. Nakada, S., Shimizu, H. & Ohta, K. Overview of the 1990–1995 eruption at Unzen Volcano. *J. Volcanol. Geotherm. Res.* **89,** 1–22 (1999).
13. Anderson, K., Lisowski, M. & Segall, P. Cyclic ground tilt associated with the 2004–2008 eruption of Mount St Helens. *J. Geophys. Res.* **115,** B11201 (2010).
14. Scott, D. R. & Stevenson, D. J. Magma solitons. *Geophys. Res. Lett.* **11,** 1161–1164 (1984).
15. McKenzie, D. The generation and compaction of partially molten rock. *J. Petrol.* **25,** 713–765 (1984).
16. Michaut, C., Bercovici, D. & Sparks, R. S. J. Ascent and compaction of gas-rich magma and the effects of hysteretic permeability. *Earth Planet. Sci. Lett.* **282,** 258–267 (2009).
17. Watts, R. B., Herd, R. A., Sparks, R. S. J. & Young, S. R. Growth pattern and emplacement of the andesitic lava dome at Soufrière Hills Volcano, Montserrat. *Geol. Soc. Lond. Mem.* **21,** 115–152 (2002).
18. Miller, A. D. *et al.* Seismicity associated with dome growth and collapse at the Soufrière Hills Volcano, Montserrat. *Geophys. Res. Lett.* **25,** 3401–3404 (1998).
19. Spieler, O. *et al.* The fragmentation threshold of pyroclastic rocks. *Earth Planet. Sci. Lett.* **226,** 139–148 (2004).
20. Umakoshi, K., Itasaka, N. & Shimizu, H. High-frequency earthquake swarm associated with the May 1991 dome extrusion at Unzen Volcano, Japan. *J. Volcanol. Geotherm. Res.* **206,** 70–79 (2011).
21. Klug, C. & Cashman, K. V. Permeability development in vesiculating magmas: implications for fragmentation. *Bull. Volcanol.* **100,** 58–87 (1996).
22. Saar, M. O. & Manga, M. Permeability-porosity relationship in vesicular basalts. *Geophys. Res. Lett.* **26,** 111–114 (1999).

Acknowledgements

The authors thank A. Burgisser whose comments helped improve the manuscript. This work was supported by Campus Spatial Paris Diderot and European Research Council Advanced Grant VOLDIES number 228064.

Author contributions

C.M. conceived the original model, C.M., Y.R. and D.B. developed the physical and mathematical model, Y.R. and C.M. developed the numerical model, and R.S.J.S. and C.M. made links between the model and the observations. C.M. was the lead author but all authors contributed to the writing of the paper.

Additional information

Supplementary information is available in the online version of the paper. Reprints and permissions information is available online at www.nature.com/reprints. Correspondence and requests for materials should be addressed to C.M.

Competing financial interests

The authors declare no competing financial interests.